ISIJ International, Vol. 44 (2004), No. 2, pp. 381–387

Effect of Silicon on the Interaction between Recrystallization and Precipitationin Niobium Microalloyed Steels

L. JIANG, A. O. HUMPHREYS and J. J. JONAS

Department of Mining, Metals & Materials Engineering, McGill University, 3610 University Street, Montreal, Quebec H3A 2B2, Canada.

(*Received on July 7, 2003; accepted in final form on September 17, 2003*)

The effect of Si addition on the interaction between recrystallization and precipitation was investigated in terms of the no-recrystallization temperature (T_{nr}) on three microalloyed steels containing about 0.035 mass% Nb. The T_{nr} was measured using torsion testing over the Si concentration range from 0.01 to 0.48 mass%. It was observed that the T_{nr} increased with Si level, but appeared to saturate at long interpass times. In addition, high strains reduced the influence of Si on the T_{nr}. This behaviour is attributed to the acceleration of Nb(C, N) precipitation by the addition of Si.

KEY WORDS: recrystallization; strain-induced precipitation; no-recrystallization temperature (T_{nr}); silicon addition; niobium microalloyed steel; hot deformation; HSLA steel.

1. Introduction

The appropriate employment of microalloying elements in high strength low alloy (HSLA) steels, coupled with thermomechanical processing, can provide improvements in both strength and toughness.[1–5] This is achieved by suitable manipulation of the recrystallization and precipitation phenomena that take place during deformation. Microalloying elements are present in HSLA steels as both solutes and precipitates. By suppressing austenite recrystallization, these elements act as ferrite grain refiners, thus increasing the yield strength and decreasing the impact transition temperature.

Carbonitride precipitation, especially strain-induced precipitation, depends largely on the temperature and deformation conditions, but can also be influenced by other alloying additions. Some non-precipitating elements, such as Mn and Si, can alter the activities of C and N[5–10]; that is to say, these elements can modify the effective solubility of Nb(C, N) and thereby influence the interaction between recrystallization and precipitation.

A clear understanding of this interaction involves the no-recrystallization temperature (T_{nr}), the temperature below which recrystallization cannot be completed within the interpass time range of a given multipass rolling operation. This temperature, which depends on the degree of supersaturation, is determined by the occurrence of precipitation; the latter in turn suppresses the progress of recrystallization.[11] In addition to composition, the T_{nr} is a function of strain, strain rate, interpass time and reheat temperature.[12–16] An increase in the T_{nr} allows finish rolling to be conducted at higher temperatures, which in turn enable lower loads to be developed or larger reductions to be applied without consuming additional energy.[14] Furthermore, the critical parameter for shape and dimensional control during rolling is the rolling load, *i.e.* mean flow stress, which determines the roll gap. Therefore, predicting the T_{nr} is important because it is associated with significant changes in mean flow stress.[3]

The aim of this study, in terms of the T_{nr}, was to examine the effect of Si addition on the interaction between recrystallization and precipitation in a series of Nb microalloyed steels. This work seeks to develop further understanding of the mechanisms responsible for this effect.

2. Experimental Procedure

Three Nb-bearing steels containing Si concentrations of 0.01, 0.11 and 0.48 mass% were studied in the present work; their detailed chemical compositions are displayed in **Table 1**. Multipass torsion tests, which are widely used to simulate industrial hot rolling, were employed to determine the T_{nr}. The as-received plates were machined into torsion specimens, with their longitudinal axes aligned along the

Table 1. Chemical compositions of the steels (in mass%).

	C	Si	Mn	Al	Nb	P	S	O	N
0.01Si	0.08	0.01	0.9	0.03	0.035	<0.004	0.0024	0.007	0.0048
0.11Si	0.11	0.11	1.0	0.03	0.034	<0.004	0.0029	0.005	0.0038
0.48Si	0.09	0.48	1.2	0.02	0.038	<0.004	0.0027	0.004	0.0047

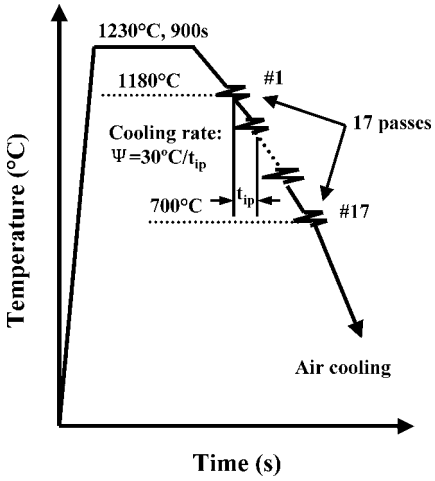

Fig. 1. Hot torsion test schedule adopted in the present work.

Table 2. Test parameters for the multipass torsion tests.

Strain/pass
ε = 0.2, 0.35
Strain rate
$\dot{\varepsilon}$ = 2/s
Interpass times
T_{ip} = 20, 30, 60, 100, 200s

rolling direction. Each specimen had a gauge length of 22.4 mm and a diameter of 6.3 mm.

The experiments were conducted using a servo-hydraulic, computer controlled MTS torsion machine. For the purpose of preventing oxidation, the specimen and parts of the loading bars were contained in a quartz tube sealed with O-rings, through which a constant flow of high purity argon was passed.

The test schedule is illustrated schematically in **Fig. 1** and the test parameters are displayed in **Table 2**. In order to avoid the occurrence of dynamic recrystallization, low pass strains were adopted. It appears from previous research[17,18] that strain rate does not have a significant influence on either the recrystallization kinetics or the T_{nr}. Thus, in the present work, all tests were conducted at a fixed strain rate of $2\,s^{-1}$. For a particular test, the pass strain and interpass time were held constant. For short interpass times (<10 s), precipitation is unlikely to take place in the early stages of multipass deformation; only solute drag retards recrystallization.[13] Therefore, the interpass times (t_{ip}) adopted in this investigation ranged from 20 to 200 s. Interpass times of 20 s are representative of reversing mills,[11] such as plate or roughing mills; thus the present results are particularly applicable to this type of mill. The temperature decrease during each interpass interval was 30°C; therefore the average cooling rates (Ψ) in the different tests were given by the relation:

$$\Psi = 30°C/t_{ip} \quad \text{.....(1)}$$

In order to reveal the prior austenite grain boundaries, sections were cut perpendicular to the radius and at a depth of $0.1r$ of the torsion samples. These were then polished and etched in saturated aqueous picric acid at 60–80°C containing several drops of hydrochloric acid and a wetting agent (detergent). The grain size was evaluated by the linear intercept method, as described in section E112 of the ASTM standards.

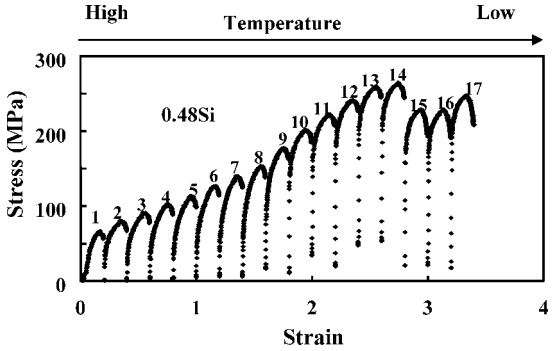

Fig. 2. Typical stress–strain curves for a 17-pass torsion test in the 0.48Si steel; $\dot{\varepsilon}=2\,s^{-1}$, $\varepsilon=0.35$, $t_{ip}=60$ s.

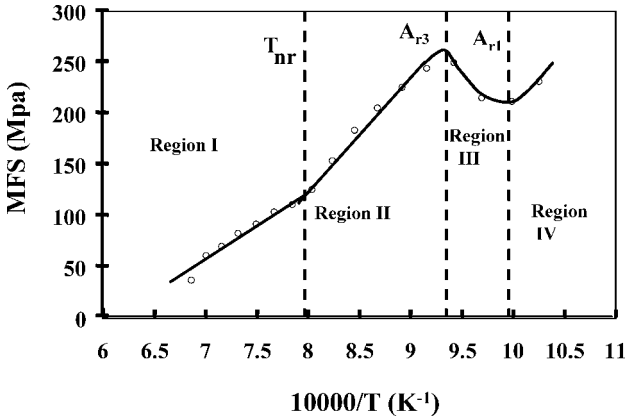

Fig. 3. Dependence of the mean flow stress (MFS) on inverse absolute temperature for the 0.48Si steel; $\dot{\varepsilon}=2\,s^{-1}$, $\varepsilon=0.35$, $t_{ip}=60$ s.

3. Results

3.1. Determination of the T_{nr}

The equivalent stresses and strains were calculated from the torque and twist data using the following equations, as employed by earlier workers[19]:

$$\sigma_{eq} = \frac{3.3\sqrt{3}\,\Gamma}{2\pi^3}, \quad \varepsilon_{eq} = \frac{r\Theta}{\sqrt{3}\,L} \quad \text{.....(2)}$$

Here, Γ is the measured torque, Θ is the measured angle of twist, r is the specimen radius, L is the gauge length. **Figure 2** shows some of the typical stress–strain curves obtained. The mean flow stress (MFS) for each pass was calculated in terms of the equivalent stress and strain by numerical integration[12]; that is:

$$\text{MFS} = \bar{\sigma}_{eq} = \frac{1}{\varepsilon_b - \varepsilon_a}\int_{\varepsilon_a}^{\varepsilon_b} \sigma_{eq}\, d\varepsilon_{eq} \quad \text{.....(3)}$$

The MFS's are plotted as a function of inverse absolute temperature in **Fig. 3**. Based on the slope change that can be seen, the continuous increase in flow stress can be divid-

ed into two regions. In region I, recrystallization takes place fairly rapidly, so that there is no accumulation of work hardening. The increase in MFS can only be attributed to the temperature drop and is thus small. In region II, the rate of change of MFS increases perceptibly. This is because only partial or no recrystallization occurs, so that the work hardening is accumulated from pass to pass. In this temperature range, the increase in MFS is due, not only to the decrease in temperature, but also to the retention of work hardening. According to Boratto *et al.*,[12] for plate rolling, the temperature corresponding to the slope change at the intersection of regions I and II can be defined as the no-recrystallization temperature (T_{nr}).

When deformation is carried out at lower temperatures, the austenite-to-ferrite transformation occurs (region III), leading to a drop in mean flow stress because ferrite is softer than austenite. In region IV, where this transformation is more or less complete, the mean flow stress increases again as a result of both strain hardening of the ferrite–pearlite structure and the decrease in temperature. The temperatures that correspond to the start and finish of this transformation can be defined as the A_{r3} and A_{r1}.

3.2. Austenite Microstructure

The deformation microstructures were examined with the aim of determining when the retardation of recrystallization occurred due to precipitation. Water quenching was performed on the 0.01Si and 0.48Si steels, according to the test schedule displayed in **Fig. 4**. The initial austenite structures for these materials are shown in **Fig. 5**. The T_{nr}'s measured for the 0.01Si and 0.48Si steels corresponding to these conditions were 938°C and 962°C, respectively. The quenching temperature used was 940°C. For the 0.01Si steel, this final temperature is above its T_{nr}, meaning that recrystallization was completed before Nb(C, N) precipitation could be initiated. Therefore, the initially large austenite grains, with an average size of 365 μm, were refined to around 50 μm (see **Fig. 6**(a)) by repeated recrystallization. However, for the 0.48Si steel, the final temperature was

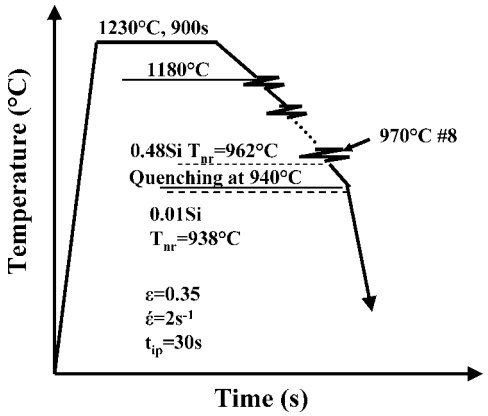

Fig. 4. Test schedule for the 0.01Si and 0.48Si steels, showing quenching point.

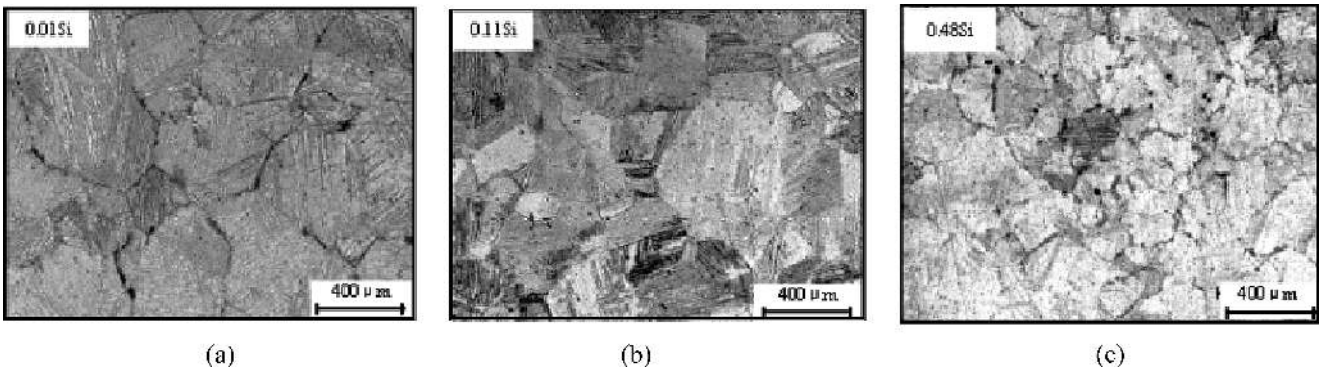

Fig. 5. Reheated austenite microstructures; soaking temperature=1 230°C, holding time=15 min.

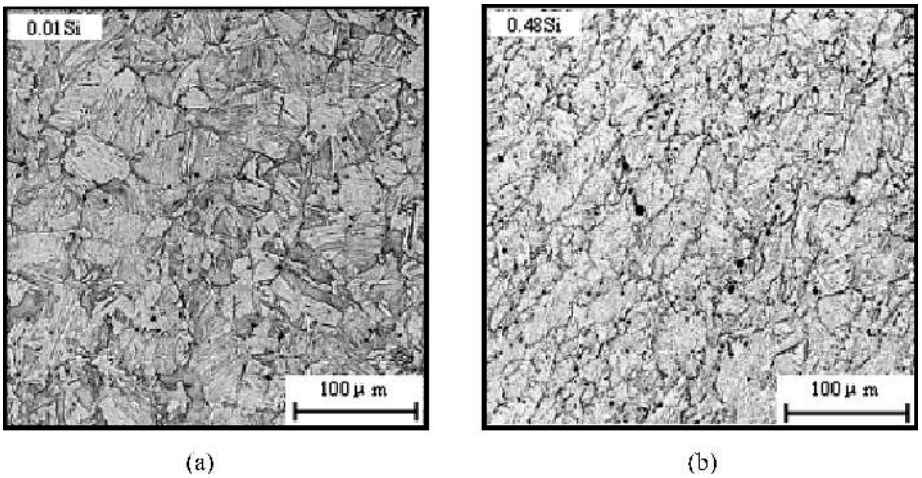

Fig. 6. Austenite grain structures in (a) 0.01Si steel and (b) 0.48Si steel; t_{ip}=30 s, ε=0.35 and $\dot{\varepsilon}$=2 s^{-1}, specimens quenched at 940°C.

below its T_{nr}; that is to say, Nb(C, N) precipitation started before quenching occurred. Thus the equiaxed grains were gradually replaced by pancaked grains, as illustrated in Fig. 6(b); this was due to suppression of the progress of recrystallization by precipitation.

3.3. Effect of Interpass Time

A set of MFS *vs.* 10 000/T curves for the 0.11Si steel is illustrated in **Fig. 7**. For these tests, the pass strain (0.35/pass) and strain rate (2 s^{-1}) were held constant and the interpass time was altered between tests (from 20 to 200 s). When deformation proceeds below the T_{nr}, the kinetics of recrystallization are retarded, whilst precipitation is accelerated. The MFS values for interpass times of 30 s are, therefore, higher than those for 20 s. However, with further increases in the interpass time, precipitate coarsening is initiated at temperatures close to the nose of the precipitation-temperature-time (PTT) curve, leading to the reduced influence of precipitation. This explains the relative positions of the MFS curves for interpass times of 30 s and >30 s in Fig. 7; here the 60 s, 100 s and 200 s MFS values are generally lower than those for interpass times of 30 s at temperatures below the T_{nr}.

The effect of interpass time on the T_{nr} for the 0.11Si steel is displayed in **Fig. 8**. For times ranging from 20 to 200 s, the diagram can be divided into two regions: precipitation and precipitate coarsening. In the precipitation region, the T_{nr} increases with interpass time until, after a certain time (for instance, around 30 s for the 0.11Si steel), the T_{nr} starts to decrease (precipitate coarsening). The dependence of the T_{nr} on interpass time in the 0.01Si and 0.48Si steels is similar to that of the 0.11Si steel, as can be seen in Fig. 8. Further interpretation of these behaviors is given in Sec. 4.

3.4. Effect of Pass Strain

Two MFS *vs.* 10 000/T plots are displayed in **Fig. 9**; these demonstrate the effect of pass strain on the T_{nr} for the 0.48Si steel. These particular specimens were tested at a constant interpass time of 20 s. It can be seen from the diagram that the MFS decreases with increasing pass strain. In addition, the point at which the slope change of the MFS *vs.* inverse temperature curve occurs moves to lower temperatures when the pass strain is increased. The influence of pass strain on the T_{nr} for the 0.48Si steel is displayed in **Fig. 10**. The results show that the T_{nr} drops with increasing pass strain in all cases.

3.5. Effect of Silicon Content

The mean flow stress *vs.* 10 000/T curves for the steels with the three different Si contents are presented in **Fig. 11** at a similar pass strain (0.2/pass) and interpass time (20 s).

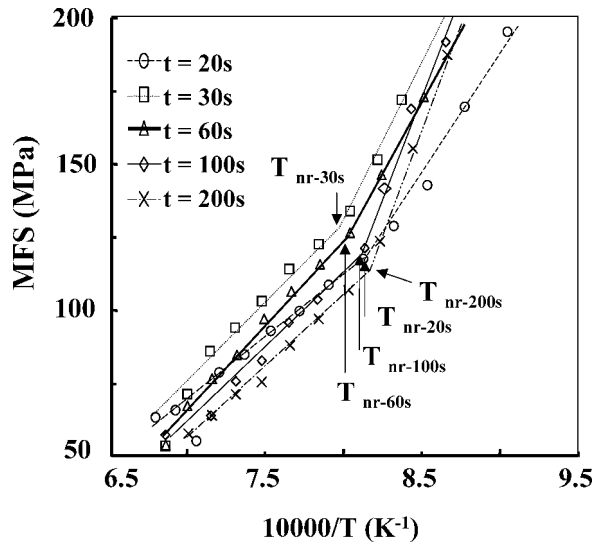

Fig. 7. Dependence of mean flow stress (MFS) on inverse absolute temperature for the 0.11Si steel; ε=0.35, $\dot{\varepsilon}$=2 s^{-1}.

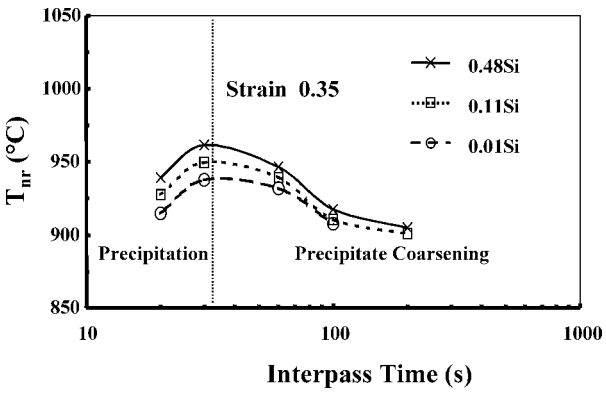

Fig. 8. Dependence of the T_{nr} on interpass time.

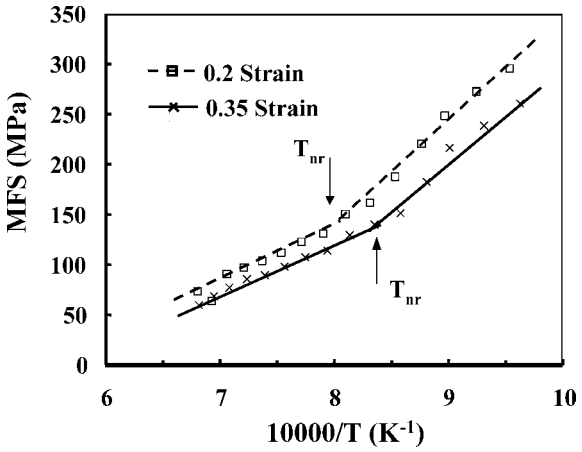

Fig. 9. Dependence of the mean flow stress (MFS) on inverse absolute temperature determined at two different pass strains for the 0.48Si steel; $\dot{\varepsilon}$=2s^{-1}, t_{ip}=20 s.

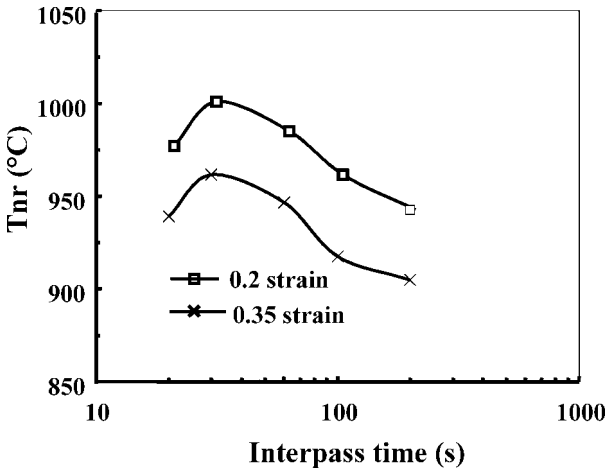

Fig. 10. Dependence of the T_{nr} on interpass time for two different pass strains in the 0.48Si steel.

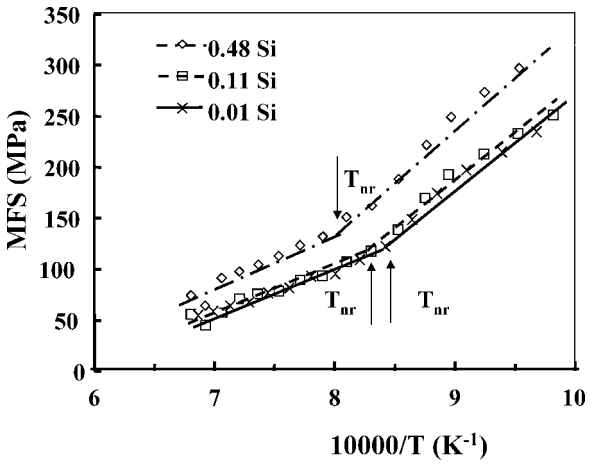

Fig. 11. Dependence of the mean flow stress (MFS) on inverse absolute temperature; ε=0.2, $\dot{\varepsilon}$=2 s^{-1}, t_{ip}=20 s for various Si levels.

It can be seen that the mean flow stress increases with Si concentration from 0.11 to 0.48 mass%. The rate of increase, however, varies greatly with interpass time and pass strain, as shown in **Fig. 12**. When relatively short interpass times were used, involving the early stages of precipitation, the increase in T_{nr} with Si content was evident. These times correspond to those conventionally employed in reversing mills. However, this effect seemed to saturate at longer interpass times. Under these conditions, there is no additional increase in T_{nr} with Si content. Such long interpass times are not encountered in typical rolling schedules. In addition, it should be noted that the extent of the increase in T_{nr} with Si level decreases when the pass strain is raised from 0.2 to 0.35, as displayed in Fig. 12.

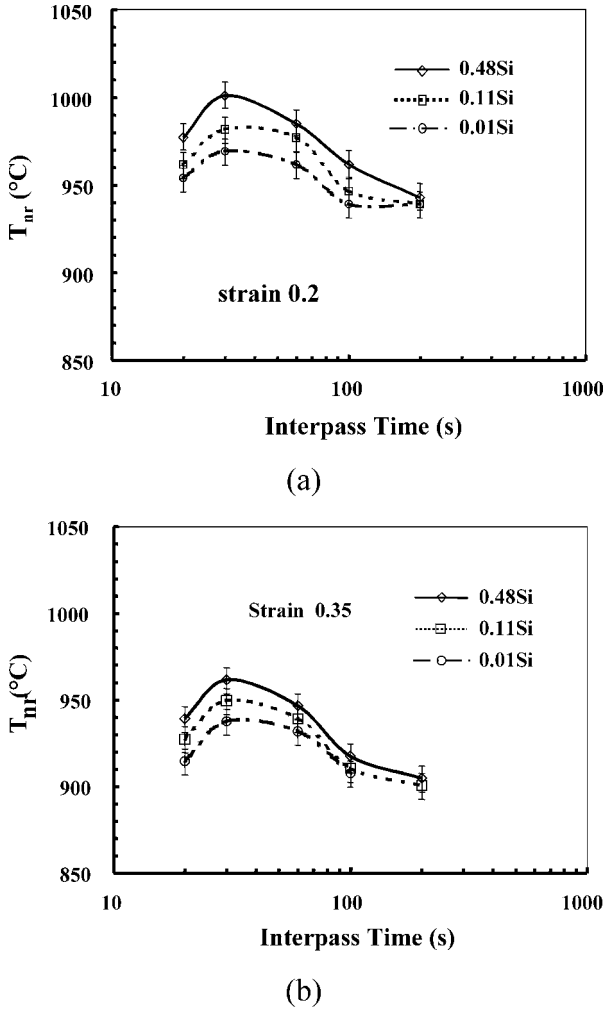

Fig. 12. Dependence of T_{nr} on Si concentration at pass strains of (a) 0.2 and (b) 0.35.

4. Discussion

4.1. Interaction between Recrystallization and Precipitation

Interpass time has an important effect on the interaction between recrystallization and precipitation as it determines whether the precipitation of microalloy carbonitrides is possible and which type of recrystallization (static, metadynamic, *etc.*) can take place.[11] Previous researchers have shown that the presence of dislocations promotes the nucleation, growth and coarsening of precipitates.[20–24] The coarsening of large precipitates at the expense of smaller ones is controlled by the diffusion of solute atoms between them. Dutta *et al.*[23] proposed that nucleation takes place at dislocation nodes in the three-dimensional dislocation network introduced by deformation, as illustrated in **Fig. 13**. Due to the acceleration of solute diffusion between particles by pipe diffusion, coarsening can readily take place. According to Dutta *et al.*,[23] coarsening starts at an early stage of precipitation and thereby leads to a substantial decrease in the precipitate number density. In addition, precipitate growth and coarsening take place simultaneously during precipitation.

The results of the present work agree very well with this model. As can be seen from Fig. 8, in the precipitation region, recrystallization is retarded to a significant degree by the occurrence of strain-induced precipitation and the T_{nr}

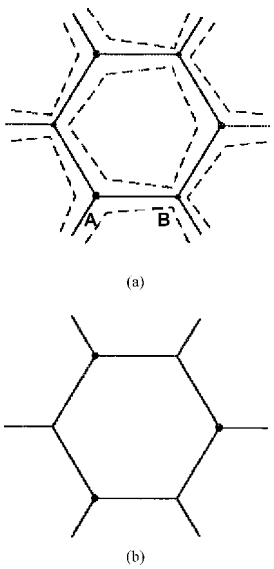

Fig. 13. Schematic diagram illustrating the distribution of particles on dislocation nodes and solute depleted zones when accelerated pipe diffusion takes place along dislocations (a) after particle growth and (b) after further growth and coarsening.[22] Note that particle B of Fig. 13(a) has disappeared in Fig. 13(b) and that particle A has coarsened.

increases with interpass time. Raising the interpass time increases the volume fraction of precipitates, thus enhancing the retardation of recrystallization by particle pinning until the interpass time reaches a critical value. At longer interpass times, particle coarsening leads to a decrease in the grain boundary pinning force; recrystallization can therefore continue to proceed until new precipitates provide additional pinning at lower temperatures. Thus, the T_{nr} decreases with increased interpass time in the precipitate coarsening region.

The interaction between recrystallization and precipitation is also strongly dependent on strain. It is well known that the time required for 50% recrystallization to occur, $t_{0.5x}$, decreases with an increase in strain, through a relationship that can be expressed as:

$$t_{0.5x} \propto \varepsilon^{-m} \quad \text{.....(4)}$$

The value of the coefficient m, according to Fernandez *et al.*,[25] varies between 2 and 4 for austenite grain size ranges of 20–1 000 μm in steels with chemical compositions similar to those of the present work. The start time for strain-induced precipitation is also reduced by increasing the strain. A relationship between the precipitation start time ($t_{0.05p}$) and strain has been determined for Nb microalloyed steels[21] to be:

$$t_{0.05p} \propto \varepsilon^{-1} \quad \text{.....(5)}$$

The rates of change of $t_{0.5x}$ and $t_{0.05p}$ with strain can be expressed by the first partial derivatives of Eqs. (3) and (4):

$$\frac{\partial t_{0.5x}}{\partial \varepsilon} \propto -m\varepsilon^{-m-1} \quad m \approx 2\text{–}4 \quad \text{.....(6)}$$

$$\frac{\partial t_{0.05p}}{\partial \varepsilon} \propto -\varepsilon^{-2} \quad \text{.....(7)}$$

Since dislocations can be nucleation sites for both recrystallization and precipitation, the increase in dislocation density resulting from increased strain accelerates the rates of both processes. Nevertheless, as displayed in Fig. 10, the T_{nr} decreases as the strain is increased. This is because the rates of acceleration for the two phenomena are different. By comparing Eqs. (5) and (6), it can be seen that the precipitation kinetics are less sensitive to strain than the recrystallization kinetics, although this difference is gradually reduced as the strain approaches unity. Furthermore, an increase in dislocation density also leads to more rapid precipitate coarsening. When these coarsened particles lose their effectiveness in pinning the grain boundaries, recrystallization is able to proceed at lower temperatures.

4.2. Effect of Silicon

Figure 12 clearly demonstrates that the influence of Si on raising the T_{nr} is not constant for different interpass times and pass strains. There are two mechanisms that can be responsible for this effect.

a) Solute Drag Effect

Bai and co-workers[13] demonstrated that, even in the absence of Nb(C, N) precipitation, a T_{nr} can still be measured at short interpass times as a result of the inhibition of recrystallization by Nb solute drag. In their recent investigation regarding the effect of Si on austenite recrystallization, Serajzadeh and Taheri[27] observed that increasing the Si concentration in plain carbon steels can increase the incubation time and decrease the growth rate of static recrystallization.

On the other hand, Mavropoulos and Jonas[28] observed that Mn in solution has an almost negligible direct solute drag effect on the migration of grain boundaries. Similarly, in the work of Akben *et al.*,[7] it was shown that a Nb HSLA steel containing 1.90 mass% Mn had a slightly lower peak strain in dynamic recrystallization than a steel of similar composition, but containing only 1.25 mass% Mn. A reasonable explanation could be that, although Mn and Si do not make direct contributions to solute drag, they may exert indirect effects by influencing the diffusivity of Nb in austenite.[8] A somewhat similar explanation has been proposed in the work of Boratto *et al.*.[3,12] They postulated that increasing the Si content has a negative effect on the T_{nr} because Si decreases the solubility of Nb(C, N) in austenite, thereby leading to a decrease in the Nb solute drag.

b) Pinning Effect due to Strain-induced Precipitation

In addition to the key role of site density in determining the precipitation kinetics of heterogeneous nucleation, the effects of alloying elements such as Si and Mn on the solubility of Nb are also important. Mn decreases the rate of Nb(C, N) precipitation,[7] in contrast to the effect of Si. This is because Si addition increases the apparent concentrations of C and N, and therefore the apparent solubility product of Nb(C, N).[9] It is well known that the occurrence of precipitation is affected by the supersaturation level of Nb(C, N), which increases as the temperature is decreased during deformation. High levels of supersaturation increase the driving force for precipitation and thereby enable precipitation to start at higher temperatures. This suppresses recrystallization at higher temperatures, which in turn increases the T_{nr}.

The increase in T_{nr} with Si level can either be caused by an increase in solute Si content in the matrix or by the enhanced precipitation of Nb(C, N). The solute Si drag effect is, however, relatively small compared with the inhibition produced by the strain-induced precipitation of Nb(C, N).[21,29] Therefore, Si is not considered as severe a recrystallization inhibitor as Nb, even though it has an effect on the kinetics of recrystallization when presents in the absence of solute Nb.[27] Once the strain-induced precipitation of Nb(C, N) takes place, the effect of Si in solid solution can be neglected. In other words, when Si coexists with Nb in steel, its influence on the progress of recrystallization is not directly attributable to the presence of Si in solution, but via its effect on the kinetics of Nb(C, N) precipitation.

If the effect of Si in raising the T_{nr} were due to the presence of Si in solution in the matrix, then the influence of Si on the T_{nr} would not vary with interpass time. When Si coexists with niobium in steel, the tendency for Si to form carbides or nitrides is small, due to the strong affinity of Nb for C and N. Therefore, whatever the interpass time, the solute Si content in the matrix should remain constant. However, from the appearance of the T_{nr} curve displayed in Fig. 12, it can be seen that the degree of increase in the T_{nr} with Si content varies for different interpass conditions. As mentioned in the previous sections, increased interpass

times correspond to the progressive occurrence of precipitate coarsening. When Nb(C, N) precipitates fail to retard recrystallization due to their coarseness, the effect of Si on the T_{nr}, through its effect on the solubility of Nb(C, N), is also eliminated.

Furthermore, in their study of a 0.084C–0.015N–0.06Nb (all mass%) steel, Dutta *et al.*[30] noted that, in a deformed material, the precipitate number density (N_v) reaches a maximum at a very early stage of precipitation and then drops soon afterwards, even though concurrently the precipitate volume fraction is still increasing. This differs from precipitation in strain-free austenite, where the maximum in N_v is only reached when precipitation is nearly finished, *i.e.* in the final stages of precipitation. It is evident that, in deformed austenite, the critical parameter that determines the effectiveness of the pinning effect of strain-induced precipitation is the number density. Therefore, an increase in the T_{nr} due to precipitate pinning can only be observed when N_v increases. The current work is consistent with this theory. At longer interpass times, although the addition of Si to Nb microalloyed steels can raise the volume fraction of Nb(C, N) precipitates, the precipitate number density decreases even though precipitation is still progressing. This has the net result of decreasing the T_{nr}.

4.3. Effect of Silicon Addition in the Presence of Other Carbide Forming Elements

Synergistic effects have also been observed when Si and V are both present in a steel in the absence of other carbonitride forming elements.[9] Si decreases the solubility of V carbide in both austenite and ferrite by raising the C activity. However, when Si coexists with other carbide-forming elements, some additions have an influence opposite to that of Si, as they decrease the activity of C. Thus, when other carbide-forming elements (such as Cr and Mo) coexist with Si, the overall combination can lead to little or no effect on the solubility of V carbide or Nb carbonitride. It has been reported that in V steels containing large amounts of other carbide-forming additions, no effect of Si on V precipitation was observed.[31] Based on the view that Si has similar effects on the solubilities of both Nb and V carbide, it is expected that Si would have no effect on the T_{nr} in Nb steels containing large amounts of other carbide-forming elements.

5. Conclusions

(1) Over a certain interpass time range ($20\,s < t_{ip} < 200\,s$), the T_{nr} increases with Si content. That is to say, in steels containing both Si and Nb additions, precipitation is capable of retarding recrystallization at higher temperatures than in steels containing only Nb.

(2) In opposition to the conclusions drawn from previous research on microalloyed steels, where the Nb remained in solution, the positive effect of Si addition on the T_{nr} is due to the indirect effect of Si on the kinetics of Nb(C, N) precipitation.

(3) The increase in T_{nr} associated with Si addition is not constant under different deformation conditions. When the interpass times are short ($20\,s \leqslant t_{ip} \leqslant 30\,s$), as in reversing mills, the T_{nr} increases with interpass time and Si content. The effect of Si on the T_{nr} appears to saturate at very long interpass times; the latter are beyond those employed industrially.

(4) Increasing the pass strain appears to accelerate the recrystallization kinetics more than the precipitation kinetics. This may be because an increase in dislocation density leads to more rapid coarsening of the precipitates. As a result, the increase in T_{nr} associated with Si addition decreases at high pass strains.

Acknowledgements

This study was supported by the Natural Sciences and Engineering Research Council of Canada (NSERC). The authors express their gratitude to The Metals Technology Laboratories of CANMET for supplying the experimental materials.

REFERENCES

1) E. C. Bain and H. W. Paxton: Alloying Elements in Steel, ASM, Metals Park, Ohio, (1961), 58.
2) R. K. Amin and F. B. Pickering: Proc. Int. Conf. Thermomechanical Processing of Microalloyed Austenite, ed. by A. J. DeArdo, G. A. Ratz and P. J. Wray, AIME, Pittsburgh, PA, (1982), 59.
3) S. Yue and J. J. Jonas: *Mater. Forum*, **14** (1990), 245.
4) L.L. Teoh: *J. Mater. Process. Technol.*, **48** (1995), 475.
5) F. Siciliano, Jr. and J. J. Jonas: *Metall. Mater. Trans. A*, **31A** (2000), 511.
6) S. Koyama, T. Ishii and K. Narita: *J. Jpn. Inst. Met.*, **35** (1971), 698.
7) M. G. Akben, I. Weiss and J. J. Jonas: *Acta Metall.*, **29** (1981), 111.
8) S. Kurokawa, J. E. Ruzzante, A. M. Hey and F. Dyment: *Met. Sci.*, **17** (1983), 433.
9) K. Han: *Scripta Metall.*, **28** (1993), 699.
10) J. X. Dong, F. Siciliano, Jr., J. J. Jonas, W. J. Liu and E. Essadiqi: *ISIJ Int.*, **40** (2000), 613.
11) J. J. Jonas: *Mater. Sci. Forum*, **284–286** (1998), 3.
12) F. Boratto, R. Barbosa, S. Yue and J. J. Jonas: THERMEC-88 Conf. Proc., ed. by I. Tamura, ISIJ, Tokyo, (1988), 383.
13) D. Q. Bai, S. Yue, W. P. Sun and J. J. Jonas: *Metall. Trans. A*, **24A** (1993), 2151.
14) R. Abad, B. Lopez and I. Gutierrez: *Mater. Sci. Forum*, **284–286** (1998), 167.
15) R. Abad, A. I. Fernandez, B. Lopez and J. M. Rodriguez-Ibabe: *ISIJ Int.*, **41** (2001), 1373.
16) M. Gomez, S. F. Medina, A. Quispe and P. Valles: *ISIJ Int.*, **42** (2002), 423.
17) A. Laasraoui and J. J. Jonas: *Metall. Trans. A*, **22A** (1991), 151.
18) D. Q. Bai, S. Yue, T. Maccagno and J. J. Jonas: *ISIJ Int.*, **36** (1996), 1084.
19) S. L. Semiatin, G. Lahoti and J. J. Jonas: Application of Torsion Testing to Determine Workability, ASM Metals Handbook, 9th Ed., Vol. 8, ASM, Metals Park, Ohio, (1985), 154.
20) H. L. Andrade, M. G. Akben and J. J. Jonas: *Metall. Trans. A*, **14A** (1983), 1967.
21) B. Dutta and C. M. Sellars: *Mater. Sci. Technol.*, **3** (1987), 197.
22) C. M. Sellars: *Mater. Sci. Technol.*, **6** (1990), 1072.
23) B. Dutta, E. Valdes and C. M. Sellars: *Acta. Metall. Mater.*, **40** (1992), 653.
24) E. J. Palmiere, C. I. Garcia and A. J. DeArdo: *Metall. Mater. Trans. A*, **25A** (1994), 277.
25) A. I. Fernandez, B. Lopez and J. M. Rodriguez-Ibabe: *Scr. Mater.*, **40** (2000), 95.
26) W. M. Rainforth, M. P. Black, R. L. Higginson, E. J. Palmiere and C. M. Sellars: *Acta Mater.*, **50** (2002), 735.
27) S. Serajzadeh and A. K. Taheri: *Mater. Lett.*, **56** (2002), 984.
28) L. T. Mavropoulos and J. J. Jonas: *Can. Metall. Q.*, **28** (1989), 159.
29) C. Ouchi, T. Okita, M. Okado and Y. Noma: Proc. Int. Conf. on Steel Rolling, ISIJ, Tokyo, (1980), 1272.
30) B. Dutta, E. J. Palmiere and C. M. Sellars: *Acta Mater.*, **49** (2001), 784.
31) F. A. Khalid and D. V. Edmonds: Proc. Int. Symp. on Microalloyed Bar and Forging Steels, ed. by M. Finn, CIM, Montreal, (1990), 1.